JMEPEG (2007) 16:321–326
DOI: 10.1007/s11665-007-9051-1

1059-9495/$19.00

Determination of Active Slip/Twinning Modes in AZ31 Mg Alloy Near Room Temperature

Hualong Li, Emilie Hsu, Jerzy Szpunar, Ravi Verma, and Jon. T. Carter

(Submitted January 4, 2007; in revised form 1 February 2007)

In order to determine the deformation modes in AZ31 magnesium alloy at room temperature, computer simulations of deformation texture development and calculation of formability have been carried out. The simulation results were compared with the measured texture results. Based on agreement between the experiments and simulations the active deformation modes were determined. A Visco Plastic Self Consistent model was employed for the simulation of plastic deformation. Simulations and experiments were performed for different initial textures. The goal of the study was to develop the understanding of deformation texture evolution and its effects on mechanical properties of magnesium, with an ultimate goal of improving room temperature formability of magnesium alloys.

Keywords deformation, formability, Mg alloy, plasticity, simulation, texture

1. Introduction

In recent years, magnesium alloys have attracted increasing interest due to their low density and high specific strength. They are being considered as potential replacements for heavier materials like steel and aluminum. However, magnesium alloys do not possess good room temperature formability (Ref 1) and forming at high temperature entails additional cost. There is considerable interest in improving room temperature formability of magnesium by microstructure and texture modifications. This requires identifying and understanding the role of different deformation mechanisms active at room temperature. The deformation mechanisms under recent consideration include slip and twinning, but may also include grain boundary sliding, which has gained increased attention (Ref 2-8). In this paper, however, only slip and twinning mechanisms were considered for deformation at room temperature.

During Mg deformation, texture evolution depends on slip/twinning activity. By comparing experimental and simulated textures, the active slip and twinning modes and their relative critical resolved shear stress (CRSS) values can be determined. It is generally agreed that the basal slip mode has the lowest CRSS and is active during room temperature deformation. However, basal slip only provides two independent slip systems. Other slip systems or twinning modes must be activated in order to deform magnesium plastically. The results of previous studies (Ref 9-11) point to the activation of additional slip modes at room temperature. Researchers (Ref 10) using the Taylor plasticity model found that a higher number of slip systems must be activated at room temperature in order to have good texture agreement with experimental results. It was found that the ⟨c+a⟩ slip mode in addition to basal slip was activated in Mg-3%Li alloy at room temperature that led to the split basal pole texture under plane strain compression (Ref 11).

In this paper, three specimens with completely different initial textures were investigated. The texture evolutions were systematically studied with increasing plastic strain. The comparisons between experimental and simulated results were used to determine and verify the active slip and twinning modes in AZ31 alloy at room temperature. The simulation results were further used to predict the room temperature ductility exhibited by the different specimens experimentally.

2. Texture Evolution and Active Slip and Twinning Modes

2.1 Computer Simulation and Experimental Methodologies

Computer simulations were based on the VPSC (Visco Plastic Self Consistent) model (Ref 12). In this model, the specimen was represented by a number of grains. The orientations of these grains were defined in such a way that they reproduced the initial texture of the specimen. Each grain was treated as an inclusion embedded in an effective medium. The effective medium represented the matrix with which each grain interacts. Thus, the grains did not interact with each other directly. Each grain, dependent on its own visco-plastic compliance or stiffness, experienced a strain or stress different from that of the medium. Deformation took place by slip and twinning, activated when the resolved shear stress exceeded the corresponding CRSS. Twinning was simulated in a manner similar to slip and differed from slip only in its directionality.

This article was presented at Materials Science & Technology 2006, Innovations in Metal Forming symposium held in Cincinnati, OH, October 15-19, 2006.

Hualong Li, Emilie Hsu, and **Jerzy Szpunar,** Department of Metals and Materials Engineering, McGill University, 3610 University, H3A 2B2 Montreal, QC, Canada. Contact e-mail: hualong.li@mcgill.ca. **Ravi Verma,** and **Jon. T. Carter,** Materials & Processes Laboratory, General Motors R&D, Warren, MI 48090.

Twinning was activated only if the resolved shear stress was positive (along the Burgers vector of the twin). The twinning process will also cause a rigid orientation flip of grains which was controlled by the Predominant Twin Reorientation Scheme (PTR) proposed by Tomé et al. (Ref 13). The main idea of PTR is that once the twin fraction reaches a certain level, one grain will be randomly chosen to flip its orientation completely.

Three AZ31 specimens with different initial textures: random, basal fiber, and off-basal, were used in this study. The random texture specimen was obtained from an as-cast material. Basal and off-basal specimens were obtained from a rolled AZ31 plate by cutting specimens parallel to and perpendicular to the rolling plane, as shown schematically in Fig. 1. Since the rolled AZ31 plate had a fiber texture, the three orthogonal cuts produced only two different initial textures A and B/C with cuts B and C having similar textures.

The specimen with random initial texture was deformed in uniaxial compression to a strain of 20%. The texture evolution due to the 20% reduction was simulated and the results were compared with the experimental texture results of the deformed specimen. The active slip and twinning modes and the relative CRSS values for AZ31 were determined by iteratively minimizing the difference between the simulated and the experimental texture results. The obtained slip and twinning modes and CRSS values were then used to simulate texture evolution in the basal and off-basal specimens under different levels of cold reduction. Actual texture measurements were made on the basal and off-basal specimens after cold rolling to the same cold reduction levels as used in the simulation, and the comparison of the simulated and experimental textures was used to further verify the deformation modes and the CRSS values.

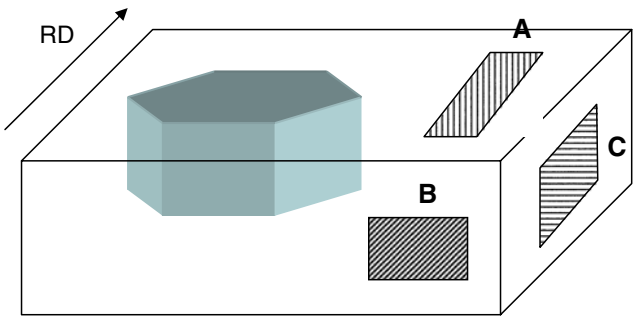

Fig. 1 Schematic illustration of specimen sectioning; basal specimen (a); off-basal specimen (b or c)

All initial and deformed textures were measured using a Siemens DX-500 X-ray diffractometer. Experimental and simulated pole figures and Orientation Distribution Function (ODF) were analyzed using TexTools software. ODFs served as input to the simulation program and were also used to represent the output of the computer simulation. From an ODF, pole figures were generated and compared to the experimental pole figures.

2.2 Texture Representation for Simulation of Plastic Deformation

Agreement between the simulated and the experimental textures was used to determine active slip and twinning systems. Therefore, the initial textures of computer-generated specimens must be quantitatively described and should agree with experimental textures. A total of 10,000 grains were used to build each computer specimen. These grains were assigned different orientations to represent the experimental texture expressed in terms of the volume fraction (dV) of grains having orientation within the orientation space element dg.

$$\frac{dV}{V} = f(g)dg, \qquad \text{(Eq 1)}$$

where V is the normalized total volume of the specimen, $f(g)$ is the ODF and the dg is the orientation element. The orientation of grains is described using Euler angles defined according to Bunge's notation (Ref 14)

$$dg \equiv d(\varphi_1, \Phi, \varphi_2) = 1/8\pi^2 \sin\Phi d\Phi d\varphi_1 d\varphi_2 \qquad \text{(Eq 2)}$$

It is assumed that all grains in the simulation have approximately the same size. The amount of grains (10,000) was chosen because it has been shown to be sufficient to accurately reproduce the initial experimental texture.

In the case of the specimen with randomly oriented grains, the ODF used in Eq (1) had an intensity of 1 for every grain orientation. For the basal and off-basal specimens, the ODFs calculated from experimental pole figures were used. The experimental ODF of the basal specimen as shown in Fig. 2 displays a strong basal fiber texture that represents 25% volume fraction within a 15° angular deviation from basal plane. The

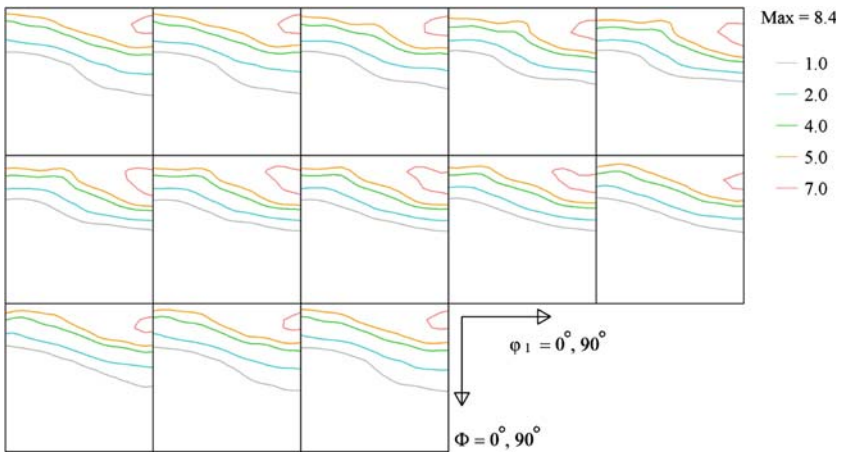

Fig. 2 Initial ODF of basal specimen calculated from experimental pole figures. φ2 cross sections from 0° to 60° with angular interval 5°

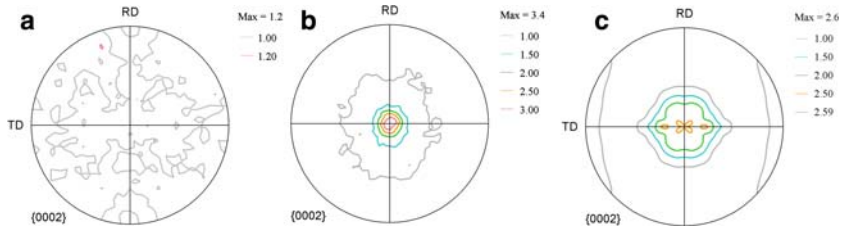

Fig. 3 Simulated and experimental texture results of specimen with random initial (as-cast) texture; (0002) pole figures: (a) simulation of initial random texture; (b) simulation at 20% compression; (c) experimental results at 20% compression (for explanation of smoothness of this pole figure read discussion)

ODF of the off-basal specimen is not shown because it had essentially the same texture but rotated 90°.

After the deformation simulation was performed, the orientation of each grain changed. The simulated ODF was then calculated from the orientations of all grains. During this calculation, hexagonal crystal symmetry and ODF domain symmetry were imposed. The resulted ODF was used to calculate pole figures and volume fractions of texture components for comparison with experimental results.

2.3 Active Deformation Modes and CRSS in AZ31

As a starting point of simulation, the basal slip and extension twinning were assumed to be active deformation modes in compression at room temperature. This assumption is based on the fact that basal fiber texture was developed and twinning activities have been observed experimentally by Barnetta et al. (Ref 15) when AZ31 was deformed at room temperature.

The CRSS ratio of basal slip and extension twinning is of the order of 1:2 (Ref 16). This ratio varies when different hardening factors are assumed. Through several iterations, a ratio of 1:3.5 was chosen which gives the best agreement with the experimental results as explained later. No hardening was assumed in the simulation.

Figure 3 shows the simulated and experimental results of the initially random texture sample. The starting texture used as input for the simulation is shown in Fig. 3(a). After 20% uniaxial compression, the simulated texture is presented in Fig. 3(b) and the experimental texture is given in Fig. 3(c). There is fairly good agreement between the simulated and experimental (0002) pole figures although the simulated pole figure had a narrower and stronger peak in the center. The volume fractions of (0002) fiber component, calculated from both the simulated and the experimental ODFs, were similar, around 11%. It should be noted that, after 20% compression the as-cast specimen still had very large grains. In order to obtain reliable statistical results, a total of four texture measurements were made at different areas of the specimen and averaged. However, the averaged pole figures were not normalized and therefore should not be used for quantitative comparison directly. Therefore, an ODF was calculated from the average pole figure, and from this 'average' ODF, the normalized pole figures were recalculated. Figure 3(c) shows the (0002) pole figure recalculated from the 'average' ODF. During the calculation, sample symmetry was imposed to improve the statistical reliability, which explains the perfect symmetry shown in Fig. 3(c).

The pyramidal ⟨c+a⟩ slip was also considered as a possible deformation mode, and was examined in simulation because it

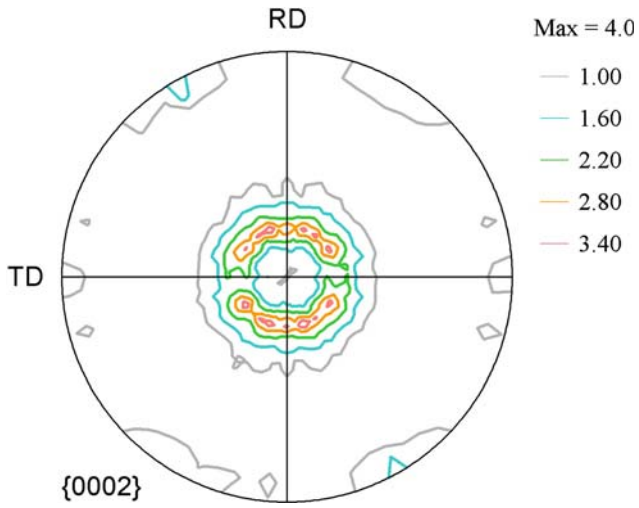

Fig. 4 Simulated (0002) pole figure at 20% compression when assuming active pyramidal ⟨c+a⟩ slip system

was found to be active at room temperature in a Mg-3%Li alloy (Ref 11). However, when the pyramidal ⟨c+a⟩ mode was assumed, the simulation disagreed with the experimental results. Figure 4 shows the simulated (0002) pole figure after 20% deformation in uniaxial compression. The initial texture of the simulation was random as shown in Fig. 3(a). The basal pole was shifted away from the center of the pole figure. The magnitude of the shift increases with the increase of the activity of ⟨c+a⟩ slip. This shift was not observed in Fig. 3(c), which represents the experimental pole figure after 20% compression. Therefore, it is concluded that the pyramidal ⟨c+a⟩ slip is not significant at room temperature. Other modes such as prismatic ⟨a⟩, pyramidal ⟨a⟩, and contraction twinning were not considered active at room temperature.

2.4 Verification of Slip and Twinning Modes

In the preceding section, the active slip and twinning modes and CRSS ratios of AZ31 alloy at room temperature were determined by fitting simulations to the experimental texture results. The specimen used for this purpose had a random initial texture, and was deformed in uniaxial compression by 20%. The results obtained were further verified by additional texture simulations of specimens with different initial textures that were cold rolled to different reduction levels. The already determined slip and twinning modes and CRSS ratios were used in these simulations and the results were then compared

with experimental pole figures. Two specimens used for the verification were basal and off-basal specimens having the orientations shown in Fig. 1.

Figure 5 illustrates the results obtained for the basal specimen. Both the simulation and the experiment started with the same initial fiber texture as shown in Fig. 5(a) and also in Fig. 2. Figure 5(b) and (c) present the simulated (0002) pole figures at 5% and 10% cold rolling reductions, and Fig. 5(d) and (e) represent experimental pole figures. Both the simulation and experimental results in Fig. 5 show that texture changed with increasing rolling reduction were small. The maximum intensities in the (0002) pole figures are between 6.6 and 7.6. The (0002) fiber volume fractions calculated from both the simulated and experimental ODFs are within a narrow range between 25% and 28%. Such a small increase in texture strength may be due to the rather small cold rolling reduction levels. Further cold rolling of the specimen was difficult due to the limited formability. Overall, it is reasonable to assume that use of identified slip and twinning modes and their CRSS values/ratios provide texture simulations that are in good agreement with the experimentally determined pole figures.

The cold rolling experiments and simulations on the off-basal specimen, which is cut from the magnesium plate as shown in Fig. 1, are carried out for up to 20% reduction. The initial texture was 90° rotated basal fiber texture as shown in Fig. 6(a). The simulated texture evolution from 5% to 20% reduction is shown in Fig. 6(b-e) and the corresponding experimental results in Fig. 6(f-i). Both simulations and experiments demonstrate that the initial basal poles shifted from TD to the center of the pole figure as the level of rolling reduction increased. This represents a change from off-basal to basal texture. During this process, both the off-basal and basal textures co-existed making the texture relatively more random. This randomization effect was observed in both the simulation and experimental results. At 10% reduction, both simulated and experimental pole figures showed a decrease in the maximum intensity of (0002) poles.

Although, texture evolution from 5% to 20% reduction shows very similar trends in the simulated and experimental pole figures, some differences can be noted. First, the maximum (0002) pole intensities in the simulated pole figures were 1.5-1.7 times higher than those in the experimental pole figures. Second, the position of the off-basal pole maxima in the simulated pole figures, indicated by 'A' in Fig. 6(d), are 10-15° displaced from those in the experimental pole figures indicated

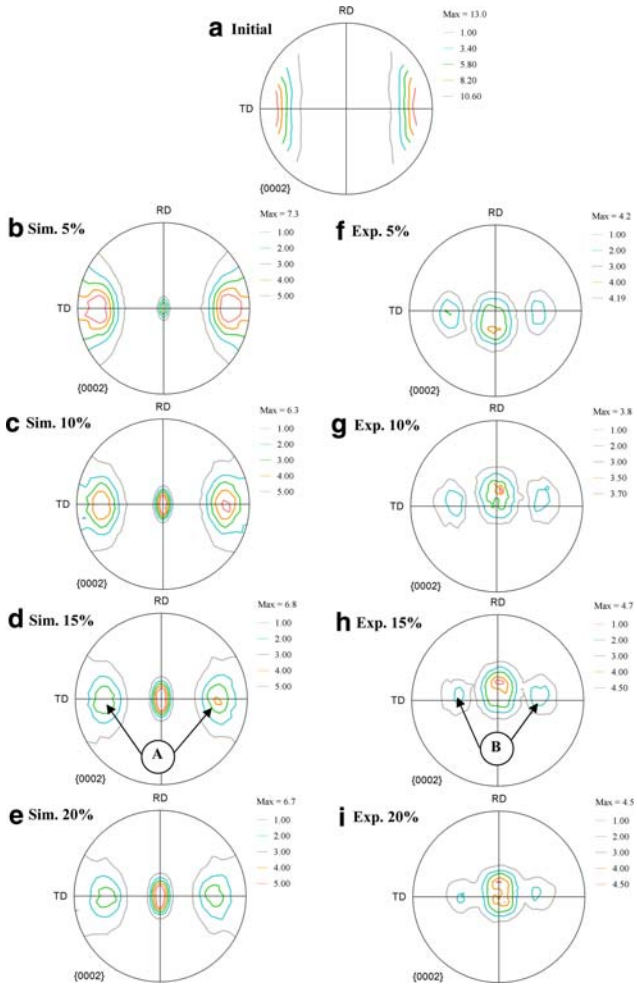

Fig. 6 Simulated and experimental rolling textures of off-basal specimen in terms of (0002) pole figures at rolling reduction levels as indicated

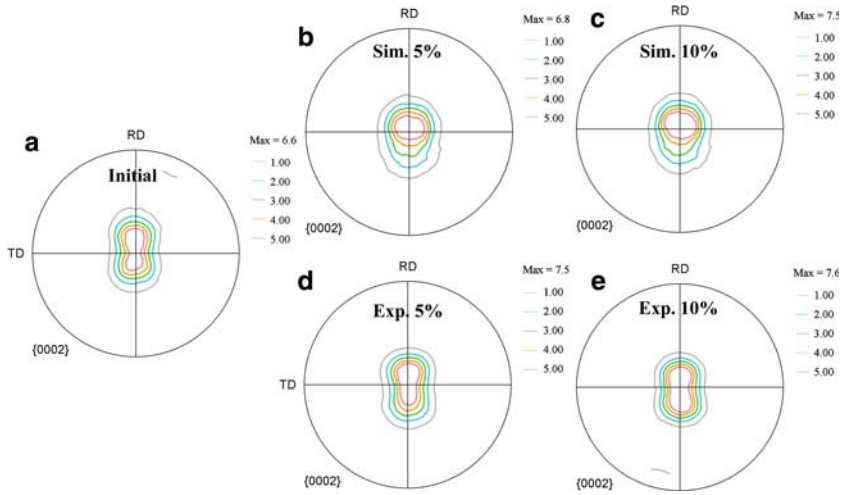

Fig. 5 Simulated and experimental rolling textures of basal specimen. (0002) pole figures of (a) initial texture; (b) simulation at 5% reduction; (c) simulation at 10% reduction; (d) experimental at 5% reduction; and (e) experimental at 10% reduction

by 'B' in Fig. 6(h). These differences are possibly due to the lack of any hardening parameters used when simulating the slip and twinning modes. The hardening effects can change the CRSS ratio of basal slip and extension twinning, and therefore can affect the texture evolution.

3. Twinning and Formability

To accommodate arbitrary shape changes of the specimen during deformation, a minimum of five independent slip and twinning systems are required. Since the basal slip mode only provides two independent slip systems, the twinning mode, which has the second lowest CRSS at room temperature, must be activated. The contributions of basal slip and extension twinning modes to the total strain are dependent on the grain orientation and the CRSS ratio, which can be calculated.

The maximum strain that can be generated by extension twinning is limited to about 7% (Ref 1) when assuming that all grains are in the most favorable orientations for twinning deformation. For polycrystalline Mg alloys with random or moderate texture, the maximum strain that can be obtained as a result of twinning alone is estimated to be about 3.5%. When ε_{33}^{twin}, which stands for strain contributed by twinning, reaches this value, the twinning activation in the specimen is saturated. Further deformation has to be supported solely by basal slip, which limits ductility and leads to fracture.

According to this analysis, the maximum amount of cold reduction a specimen with a given initial texture can undergo can be determined by tracking exhaustion of twin deformation as measured by maximum twinning strain ε_{33}^{twin}. The results are given in Fig. 7. Assuming that 3.5% is the maximum strain provided by twinning, the random specimen can be deformed to roughly 30% reduction the basal specimen to 10% and the off-basal specimen to 20% reduction. These predicted failure strains are in good agreement with the experimental failure strains of 20–25%, 11–13%, and 20% for as-cast, basal and off-basal specimens, respectively. The better formability of the as-cast specimen was due to its random texture that was favorable for the activation of basal slip and thus required less twinning contribution. The same reasoning holds for the slightly increased formability of the off-basal specimen. During the deformation of the off-basal specimen, the texture was randomized due to the changing of off-basal to basal texture, as shown in Fig. 6.

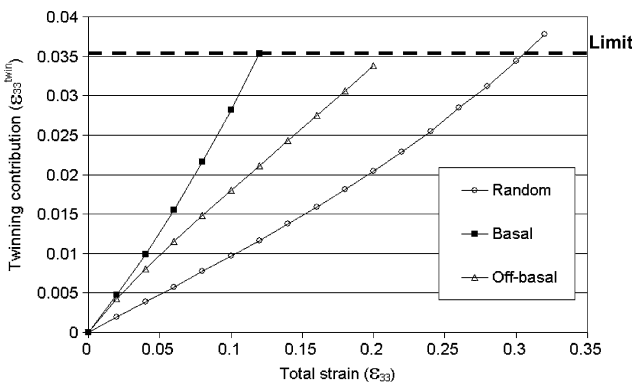

Fig. 7 Simulated twinning contribution to total strain during deformation

4. Conclusions

Simulations and experimental observations of texture evolution during room temperature deformation of AZ31 specimens with various initial textures were compared. Based on good agreement between the simulation and experimental results, it was shown that basal slip and extension twinning are the primary deformation modes of AZ31 alloy at room temperature. A CRSS ratio of 1:3.5 was established for the two deformation modes.

Simulation of pyramidal ⟨c+a⟩ slip systems did not agree with experimental results and were not considered to be active at room temperature.

It was demonstrated that the contributions of the slip and the twinning modes depend on the initial texture of the deformed specimen, and the basal slip favorable texture (e.g. random texture) is preferred to improve formability. This texture will require minimal contribution from extension twinning for deformation, and therefore can achieve better formability by spreading the twinning contribution (~3.5%) over a larger total strain.

Acknowledgments

The authors thank Paul Krajewski of GM R&D for reviewing the manuscript and for many helpful suggestions, and gratefully acknowledge the financial support from General Motors of Canada and the Natural Sciences and Engineering Research Council of Canada.

References

1. R.W. Hertzberg, *Deformation and Fracture Mechanics of Engineering Materials*, 4th ed., John Wiley & Sons, Inc, New York, 1995
2. F.A. Mohamed, The Role of Boundaries During Superplastic Deformation, *Surf. Interface Anal.*, 2001, **31**, p 532–546
3. A. Mwembela, E.B. Konopleva, and H.J. McQueen, Microstructural Development in Mg Alloy AZ31 during Hot Working, *Scripta Mater.*, 1997, **37**(11), p 1789
4. J.K. Solberg, J. Tørklep, O. Bauger, and H. Gjestland, Superplasticity in Magnesium Alloy AZ91, *Mater. Sci. Eng.*, 1991, **A134**, p 1201
5. A. Yamashita, Z. Horita, and T.G. Langdon, Improving the Mechanical Properties of Magnesium and a Magnesium Alloy Through Severe Plastic Deformation, *Mater. Sci. Eng.*, 2001, **A300**, p 142
6. H. Takuda, S. Kikuchi, and N. Hatta, Possibility of Grain Refinement for Superplasticity of a Mg-AI-Zn Alloy by Pre-deformation, *J. Mater. Sci.*, 1992, **27**, p 937
7. A. Bussiba, A.B. Artzy, S. Shtechman, and M. Ifergan, Grain Refinement of AZ31 and ZK60 Mg Alloys—Towards Superplasticity Studies, *Mater. Sci. Eng.*, 2001, **A302**, p 56
8. H. Watanabe, T. Mukai, K. Ishikawa, M. Mabuchi, and K. Higashi, Realization of High-Strain-Rate Superplasticity at Low Temperatures in a Mg-Zn-Zr Alloy, *Mater. Sci. Eng.*, 2001, **A307**, p 119
9. J.A. del Valle, M.T. Pérez-Prado, and O.A. Ruano, Texture Evolution During Large-Strain Hot Rolling of the Mg AZ61 Alloy, *Mater. Sci. Eng.*, 2003, **A355**, p 68
10. A. Styczynski, C. Hartig, J. Bohlen, and D. Letzig, Cold Rolling Textures in AZ31 Wrought Magnesium Alloy, *Scripta Mater.*, 2004, **50**, p 943
11. S.R. Agnew, M.H. Yoo, and C.N. Tome, Application of Texture Simulation to Understanding Mechanical Behavior of Mg and Solid Solution Alloys Containing Li or Y, *Acta Mater.*, 2001, **49**, p 4277
12. R.A. Lebensohn and C.N. Tome, A Self-consistent Anisotropic Approach for the Simulation of Plastic Deformation and Texture Development of Polycrystals—Application to Zirconium Alloys, *Acta Metall.*, 1993, **41**, p 2611

13. C.N. Tome, R.A. Lebensohn, and U.F. Kocks, A Model for Texture Development Dominated by Deformation Twinning Application to Zirconium Alloys, *Acta Metall. Mater.*, 1991, **39**, p 2667
14. H.J. Bunge, *Texture Analysis in Materials Science*, Butterworth, London, 1982
15. M.R. Barnetta, M.D. Navea, and C.J. Bettlesb, Deformation Microstructures and Textures of Some Cold Rolled Mg Alloys, *Mater. Sci. Eng.*, 2004, **A386**, p 205
16. C.S. Roberts, *Magnesium and its Alloys*, Wiley, New York, 1960 180